Investigation of Short-Term Intermittency in Solar Irradiance and Its Impacts on PV Converter Systems

Yuan Yao
School of Electrical & Electronic Engineering
The University of Adelaide
Adelaide, Australia
yuan.yao@adelaide.edu.au

Nesimi Ertugrul
School of Electrical & Electronic Engineering
The University of Adelaide
Adelaide, Australia
nesimi.ertugrul@adelaide.edu.au

Ali Pourmousavi Kani
School of Electrical & Electronic Engineering
The University of Adelaide
Adelaide, Australia
a.pourm@adelaide.edu.au

Increased installation of solar photovoltaic (PV) systems has drawn concerns of managing and mitigating the fast and unpredictable variations in solar power generation. This paper presents a detailed analysis of short-term (seconds level, transients) solar intermittency and its implications on solar PV array and DC/DC power converters. The impacts of the short term intermittency to the output power variations have also been studied considering the filtering components of the converter. In addition, the paper addresses the challenges about the identification of the short-term solar intermittency by utilising a moving window method. Furthermore, simulation and data analysis results provide insights of overcoming short-term solar uncertainty for PV system design and technical requirements of suitable power converters.

Keywords— Photovoltaic (PV), solar intermittency, data analysis, DC/DC converter, converter control

I. INTRODUCTION

The fast-growing solar PV penetration becomes one the most significant and urgent challenges in the context of renewable energy integration and meeting the greenhouse gas emission target. Notably, the Australian Energy Market Operator (AEMO) recently forecasts that the total capacity of the distributed PV such as rooftop is likely to reach to 69 GW level by 2050, which is nearly five times the existing capacity [1]. Within the same time frame, it is predicted that the number of large-scale solar farms will also increase drastically. Therefore, as it was observed by the reduction of power system inertia by the integration of renewable energy resources, these increasing solar PV trends are likely to lead to various other operating and coordinating problems.

Two of the problematic features of the solar PV resources are the intermittency due to the sun's position and unexpected transient fluctuations due to the cloud movements and scattering of the sun light. The former one is much slower in time (minutes level, see Fig. 1a) and commonly addressed by battery storage systems. The latter one, however, is much faster (seconds level, see Fig. 1b) and has a significant impact on the design, operation and control of the converter. It is highly critical to emphasise here that the solar irradiance exceeds 1 kW/m^2 level during scattering (Fig. 1b) hence has a potential to produce much higher voltages on the PV cells. Furthermore when the solar PV penetration gets larger and becomes a significant portion of the total power generation, unwanted fast oscillations in the solar PV system also becomes highly critical requiring a special attention.

Previous literatures mainly focused on analysing the solar intermittency and its associated impacts from the energy perspectives [2] – [4]. In the literature, the ramping rates of solar irradiance have been evaluated on an hourly or daily basis. These help to determine and to optimise the sizing of the solar PV as well as the "energy" storage systems. However, as stated previously, analysing the stochastic variations in solar within short time frames are more critical than hourly irradiance ramping for improving the operational reliability and smoothing the power flow at distribution level [5]. Although some researchers have studied the irradiance intermittency mitigation via integrating energy storage components such as batteries or electric vehicles (EVs) at short time scales [6] – [9]. However, these previous studies only dealt with the solar uncertainty at "minutes" level. Therefore, the solar variations within "seconds" need to be categorised and its potential impacts on solar PV and associated power converters output should be studied which are the aims of this research.

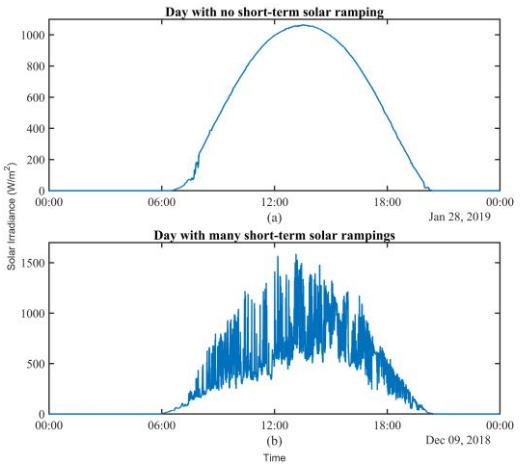

Fig. 1. Two typical days of measured solar irradiances: a) Under a full-sun, b) Under scattering of the sun light with transient fluctuations.

This paper investigates the daily solar irradiance in detail to be able to classify and identify its impacts on the design and control of the associated systems. Section II introduces the dataset used, provides statistical analysis and presents an approach using sliding window to identify the characteristic periods of short-term solar variations. Section III describes the models of solar PV and power converter control to achieve the maximum power point tracking (MPPT). Then, the simulation results with various solar intermittency conditions are presented and discussed in Section IV. Finally, the conclusion section summarises the key finding from the results.

II. SOLAR DATA ANALYSIS

The solar irradiance time series data used in this study is obtained from the project of the Australian Energy Storage Knowledge Bank (AESKB). The project has developed a mobile test platform to address the challenges of integrating

grid-scale battery storage system and integration of multiple distributed energy resources in a microgrid platform [10].

In the AESKB project, an external weather station with a pyranometer had been installed on the roof of the mobile test unit. The pyranometer provided a high resolution measurement of solar irradiance as well as the ambient temperature in 1 second sampling rate. Since this paper aims to study the impacts of solar irradiance fluctuation on power converters and associated microgrid in the future research, the summer season is selected as it is the most characteristic time period. Therefore, the solar irradiance dataset available in the test unit has covered the time period from December 2018 to the end of January 2019. Note that the data set has been obtained in Cape Jarvis, a town in South Australia, which has a significant rooftop solar PV penetration including a reverse power flow at the distribution system level.

A. Statistical Analysis

The data available has been statistically analysed as described in the following paragraphs to provide an insight on the solar irradiance variations in different time scales. As the short-term variation in solar irradiance is the major focus of this paper, the instantaneous rate-of-change of irradiance can be easily calculated as $RoCoG = dG/dt$, where G denotes the solar irradiance in unit of W/m^2.

Note that, a ramping up in solar irradiance usually follows by a ramping down with similar amplitude within a short timeframe. This can be verified by Fig. 2 which shows the relative probability distribution of *RoCoG* of the entire dataset (62 days in total). Note that the blank area in the middle part of the relative probability distribution is due to the data points that is below 10 W/m^2/s hence omitted. Note also that solar irradiance ramping rates are relatively symmetric. Therefore, the absolute value of *RoCoG* is computed to statistically analyse the data. Table I summarises the maximum, mean and standard deviation of solar irradiance and absolute valued irradiance rate-of-change over two different ramp durations.

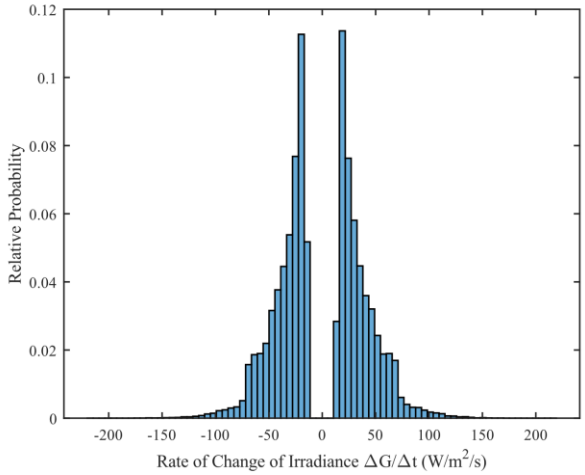

Fig. 2. Probability distribution of rate-of-change of irradiance.

TABLE I. MAXIMUM, MEAN, AND STANDARD DEVIATION OF SOLAR IRRADIACNE (W/M^2) AND ABSOLUTE VALUE OF IRRADIANCE RAMP RATE (W/M^2/S OR W/M^2/MIN)

G			**Duration**	***|RoCoG|***		
Max	***Mean***	***Std***		***Max***	***Mean***	***Std***
1669	303.7	383.2	1 sec	219.0	1.124	5.647
			1 min	999.2	27.59	90.86

To understand the relation between the short-term solar intermittency and the time of occurrence, several histograms have been produced as illustrated in Fig. 3 and 4. Noted that very small values of irradiances and their ramp rates and the evening hours have been omitted for a better visualisation.

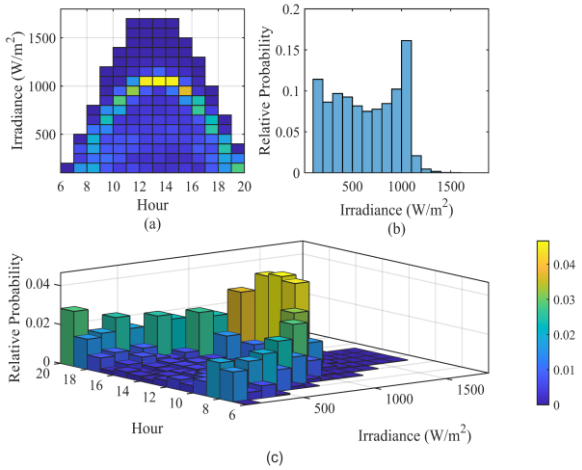

Fig. 3. Histograms of ***G*** and occurred within hours: a) Tiled view, b) Probability distribution of ***G* only** and c) Bivariate histogram.

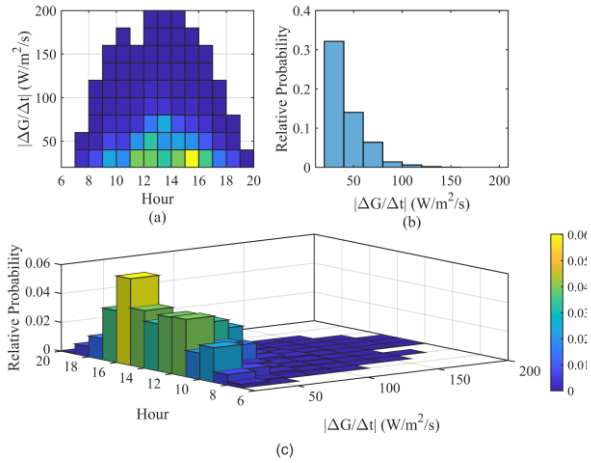

Fig. 4. Histograms of ***|RoCoG|*** and occurrances within hours: a) Tiled view, b) Probability distribution of ***|RoCoG|* only** and c) Bivariate histogram.

The two subplots in the first row of the figures are essentially the top and side views of the bottom 3-d bivariate histogram of G and $|RoCoG|$ within the recorded time frame in hours in solar timeseries data. The overall shape of Fig. 3(a) matches the normal distribution of solar irradiance over one day with good solar condition (as in Fig. 1a). In addition, Fig. 3(b) and 4(b) indicate that the irradiance itself forms uneven distribution while the absolute value of *RoCoG* follows a left-skewed distribution.

After the evaluation of the data at much longer time period, the daily max, mean and standard deviations of G and $|RoCoG|$ can be given as in Fig. 5. By applying different conditions to these aggregated parameters, some characteristic days can be extracted from the entire dataset. These include the smoothest day with negligible intermittency or the most ramping days with many fluctuations. For example, Fig. 1 displays two days of the two contrasting conditions in which the first subplot shows a sunny day without noticeable irradiance fluctuation while the second subplot demonstrations a very distorted day

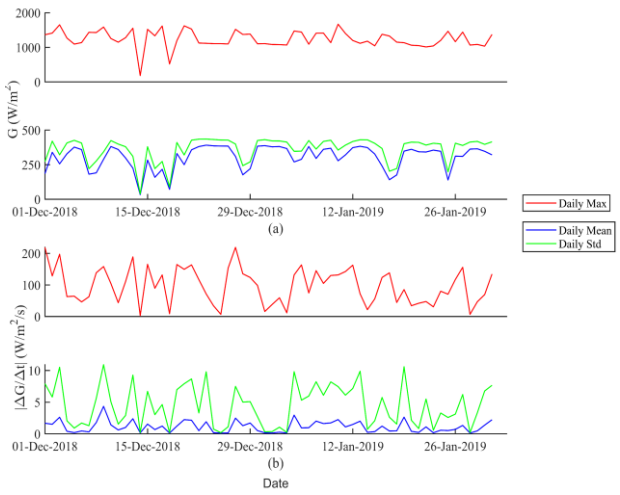

Fig. 5. Daily statistical analysis of (a) *G* and (b) |*RoCoG*|.

with many ramping events in the solar irradiance. However the detailed method of sorting out these specific days is out of the scope of this paper, hence will not be discussed further.

B. Short-term Analysis

In the above discussions, the overview of the solar intermittency distribution is presented. However, the instantaneous irradiance variations are more attracting and valuable than statistical analysis if the impacts of those intermittency towards solar PV, power converters and a DC microgrid is considered. The short-term solar intermittency can be evaluated under different time scales. Hence, the sliding window method has been employed to the timeseries to obtain the solar variations with five different window sizes (2, 5, 10, 30 and 60 s).

Equation (1) below shows how the difference between the maximum and minimum irradiance within specified moving window are computed,

$$\Delta G = \left| \max_{i=1,\ldots,n} G_i - \min_{i=1,\ldots,n} G_i \right| \quad (1)$$

where n is the length of the moving window. Noted that, n is the total number of data points contained within the sliding window. That implies the duration of each window is equal to $n - 1$. For example, when $n = 2$, the result of this equation is exactly the same as the instantaneous value of the |*RoCoG*| as there are only two data entries in the window so $\Delta t = 1$ s.

After processing of all data with the five different windows, the maximum ramping up and ramping down events within each moving window can be extracted as illustrated in Fig. 6. Note that except the first two conditions where there are six data points plotted for better visualisation, the displayed duration is twice the value of the other cases.

TABLE II. THE MAXIMUM POSITIVE AND NEGATIVE IRRADIANCE VARIATIONS OVER DIFFERENT WINDOWS

Window size (s)	**ΔG (W/m²)**	
	Up	***Down***
1	218.9	-218.8
5	550.1	-560.7
10	828.4	-824.4
30	973.1	-964.3
60	1013.0	-1012.0

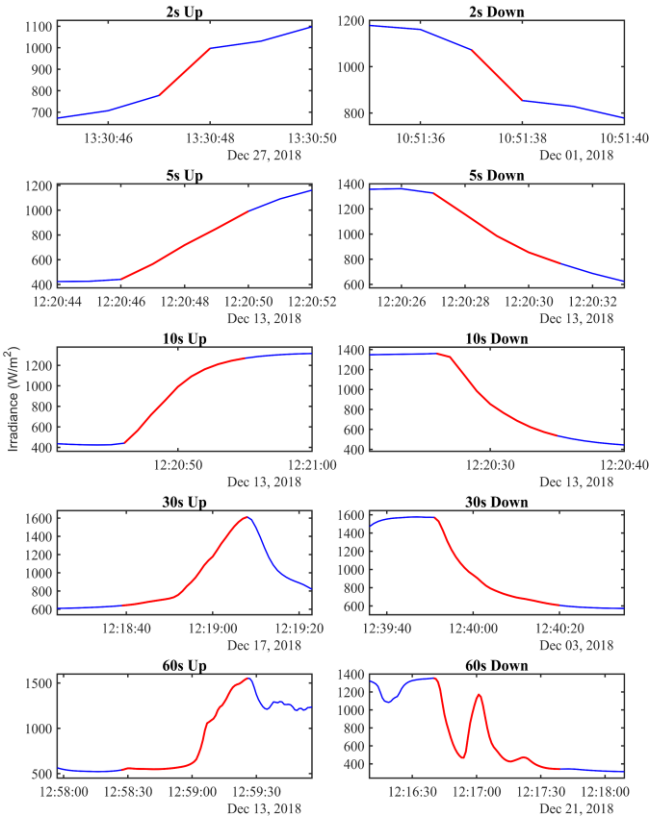

Fig. 6. The largest ramping up and down over different moving windows.

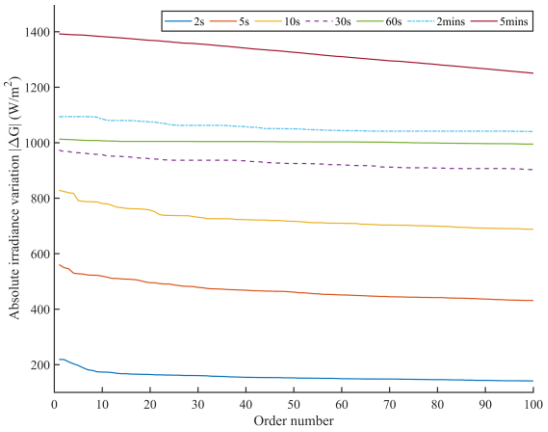

Fig. 7. Top 100 of the highest absolute irradiance variations over different windows.

The regions containing the maximum ramping up and ramping down are highlighted in red colour and centred in each subplot in Fig. 6 and the values of corresponding irradiance variations have been summarised in Table II.

Furthermore, to understand the trend and distribution of more cases, the largest 100 of positive and negative variations under seven windows (previous five windows in seconds plus two windows in 2 and 5 mins) have been aggregated by taking the absolute value as |Δ*G*| and sorted into descending order as shown in Fig. 7. This demonstrates that larger amplitude of irradiance fluctuations will be observed in longer time periods. However, the distribution of |Δ*G*| at n = 30, 60 s and 2 mins are relatively close which indicates the magnitudes of short-term irradiance variations are somehow limited around 900 to 1100 W/m^2 with repeating periods of 0.5 to 2 mins. Moreover, the varying trends of short-term intermittency presented in this

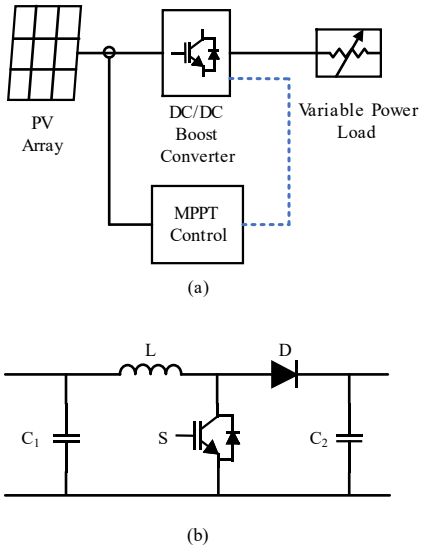

Fig. 8. The structure of a) Simulated solar PV system and b) The DC/DC boost converter topology illustrating filtering components (capacitors) that has an impact on the transient irradiances.

figure can help to quantify the variations in voltage and power generation from solar PV due to ΔG under different time scales.

III. SYSTEM CONFIGURATIONS

A standalone solar PV system with a DC/DC converter and a variable load (see Fig. 8a) has been considered to investigate the fluctuations in voltage, current and power at the output of solar PV and converter due to the transient intermittency in irradiance as discussed in previous section. The detailed models of the subcomponents of the system are necessary to accurately reflect the impacts of the short-term variations. This section outlines the specification of the solar PV, DC/DC boost converter, variable loads as well as the MPPT control of the PV generation.

To mimic a common residential PV systems, a 6 kW solar PV panel array has been considered which involved 3 parallel strings and 9 series PV modules per string. The detailed model of PV modules is adopted from the National Renewable Energy Laboratory (NREL) System Advisor Model (SAM) database [11]. The maximum power of the selected PV module is about 220 W under the standard test conditions (STC), where the irradiance is 1000 W/m^2 and the temperature

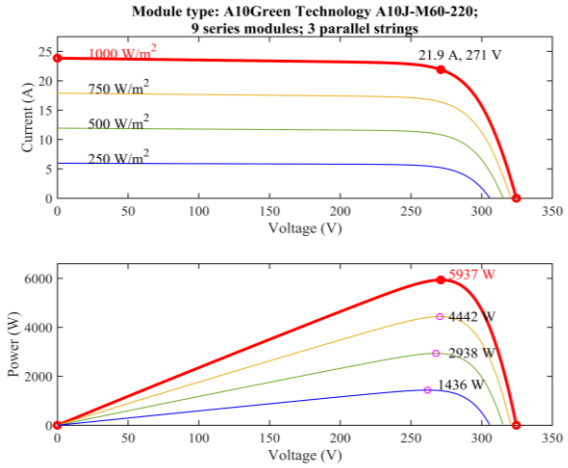

Fig. 9. Solar panel *I-V* & *P-V* characteristics under various irradiance.

is 25 °C. The *I-V* and *P-V* curves of the PV panel model has been plotted under various irradiances (250, 500, 750 and 1000 W/m^2) in Fig. 9. The maximum power points of different conditions have been labelled with a round marker on the *P-V* characteristics. Note that if the PV system (including the PV panels, the converter and the control system) responses to the transient variations of irradiances quickly, the solar PV output power can also fluctuate at kW level. Therefore, it is important to evaluate the resulting voltage, current and power fluctuations at the converter level.

The PV output is connected to a DC/DC boost converter which enables the PV to operate at the MPPT mode. The detailed circuit model of the boost converter is illustrated in Fig. 8(b). Note that the converter accommodates a MOSFET switch operated at 10 kHz switching frequency, and it has been designed to operate at the continuous conduction mode (CCM) to reduce the current ripples, increase the overall efficiency and simplify the converter control design. All component values are listed in Table III. The converter is controlled in a conventional mode by adjusting the duty cycle of PWM signal. A double-looped PI control is introduced to regulate both the solar PV output voltage and current. For the design of MPPT control, the strategy of Perturb and Observe (P&O) has been employed due to its effectiveness and simplicity [12]. The detailed design of the control system for the solar PV boost converter has been discussed under the section of the primary control in [13].

TABLE III. BOOST CONVERTER PARAMETERS

Parameters	Values
MOSFET f_{sw} (kHz)	10
Inductor L (μH)	35.4
Capacitor C_1 (μF)	3300
Capacitor C_2 (mF)	12.4

Note that since the solar PV output power changes, it is critical to capture the highest power via the MPPT control. Therefore, a dynamic load which has the capability to track the power variations due to MPPT has been modelled by a controlled current source and connected to the high voltage side of the boost converter as shown in Fig. 8(a).

IV. SIMULATION RESULTS AND DISCUSSIONS

The model of solar PV, DC/DC boost converter and the dynamic power load has been developed and simulated in MATLAB/Simulink. Firstly, the standard testing condition has been applied to the system to provide a benchmark of the solar PV performance as a reference. Table IV lists the steady-state output *V*, *I* and *P* of the PV array and DC/DC converter. Then, ten different ramping conditions presented previously have been utilised to test the solar PV response towards the short-term irradiance transients.

TABLE IV. SOLAR PV OUTPUTS UNDER STC

Component	Voltage (V)	Current (A)	Power (W)
PV Array	275.4	21.6	5937
Boost Converter	335.1	16.2	5455

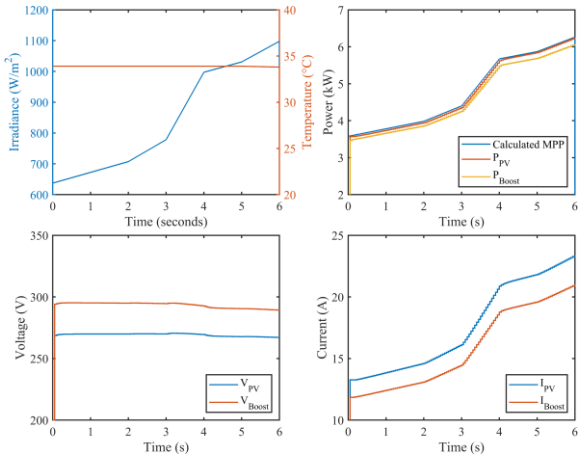

Fig. 10. The output power, voltage and current of solar PV and converter under **2 s ramping up**.

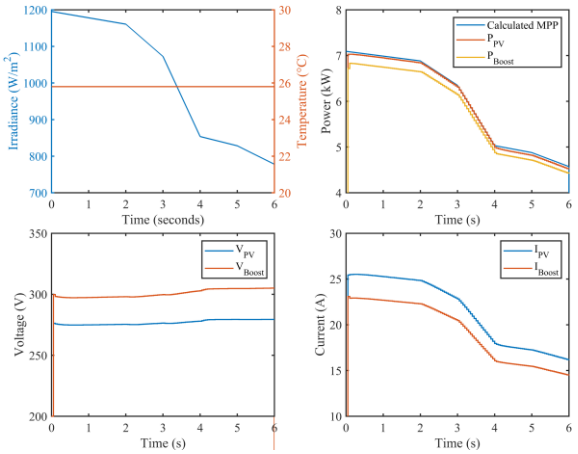

Fig. 11. The output power, voltage and current of solar PV and converter under **2 s ramping down**.

A. Case 1: Highest Ramping Up in 2 s Window

The first scenario is when the maximum instantaneous increase is identified in solar irradiance. Fig. 10 shows the system behaviour with output V, I and P of the PV and converter under this case. From $t = 3$ to 4 s, the irradiance sees a sudden rise from 778.3 to 997.2 W/m^2. Consequently, the solar PV and converter output power exhibit the same trend of variations with similar rising slope. The blue line in the power curve is the theoretical MPP using the PV equation and parameters from the NREL SAM as introduced in system configuration section. Note that the calculated MPP curve matches the red line which is the PV output power, which means that the MPP tracking has been effectively achieved by the converter control. In addition, the power generated from the boost converter is always lower than P_{pv} due to power losses in the converter. The power variations of PV and converter in this scenario are ΔP_{pv} = 1.27 kW and ΔP_{boost} = 1.22 kW respectively. At the same time, the output currents also follow the similar trend of climbing like power outputs. The current variations were found ΔI_{pv} = 4.74 A as ΔI_{boost} = 4.30 A. As the window size in this case had two data points, so that all the variations observed are the same as the rate-of-change of different parameters. On the other hand, the solar PV and converter voltages remain relatively stable compared to their current and power outputs.

B. Case 2: Highest Ramping Down in 2 s Window

In this scenario, the irradiance starts from a value that is higher than the standard condition but keeps decreasing over the entire window. As illustrated in Fig. 11, at $t = 3$ to 4 s, the most significant drop occurred with ΔG = −218.8 W/m^2. Similar to Case 1, this reduction results in noticeable dips with ΔP_{pv} = −1.32 kW, ΔP_{boost} = −1.26 kW, ΔI_{pv} = −4.87 A, and ΔI_{boost} = −4.39 A while V_{pv} and V_{boost} are not affected by the irradiance ramping. However, the magnitude of the drops in solar PV and boost converter outputs are slightly higher than the ramping up scenario given that Case 1 has nearly the same amount of irradiance variations as in Case 2. One possible reason is the air temperature difference considering the ambient temperature is T = 34 °C in first scenario while the temperature only has T = 25.8 °C in this case. Other potential aspect may relate to the modelling of PV modules and converter. Hence, this phenomenon and its causes requires further investigation.

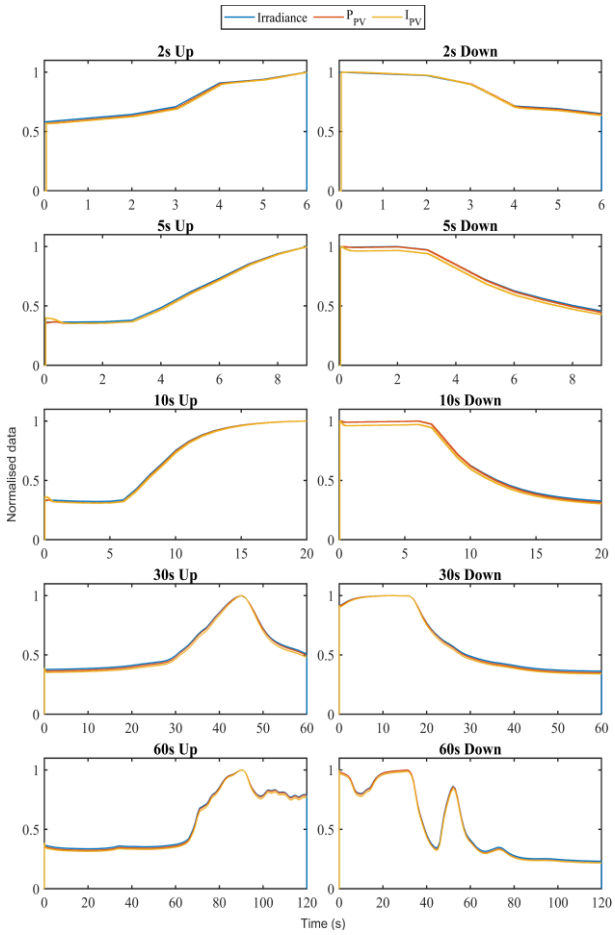

Fig. 12. Normalised variations of irrdiance, solar PV output power and current under different ramping up and down conditions.

C. Case 3: Highest Ramping in 5, 10, 30 and 60 s windows

After testing with the two most extreme conditions, the solar irradiance intermittency within couple of seconds and its impacts on the solar PV system have been studied. The rest of ramping up and ramping down cases with different window lengths are applied to the input of solar PV models. From Case and Case 2, it can be concluded that power output P_{pv} and P_{boost} as well as the current I_{pv} and I_{boost} always change in a similar manner as the solar irradiance. However the PV and converter output voltages are not sensitive to the irradiance fluctuations. Therefore, only the P_{pv} and I_{pv} under the other window sizes of 5, 10, 30 and 60 s have been plotted along with the

irradiance G as demonstrated in Fig. 12. Noted that the vertical scales have been normalised to per-unit values for better visualisation.

After simulating all ten conditions with five moving windows, the largest amount of variations in P_{pv}, P_{boost}, I_{pv} and I_{boost} over different windows as well as the maximum rate-of-change of these parameters have been obtained and summarised in Table V. The first five columns with values are the maximum variations in irradiance, power and current over its sliding window while the last five columns list the detected maximum rate-of-change. Note that the data for 5 s window has been omitted due to both of the ramping up and down cases are detected at the same periods as in the 10 s scenarios. Thus, the ramping rates are also identical as n = 10 s. The shaded sections in the row of 2 s highlight the maximum of the absolute value of ramping rates of $\Delta G/\Delta t$, $\Delta P_{pv}/\Delta t$, $\Delta P_{boost}/\Delta t$, $\Delta I_{pv}/\Delta t$ and $\Delta I_{boost}/\Delta t$. Note that these values are not only the highest ones within this specific window, but also the maximum possible rate-of-change of those parameters over the entire dataset. Hence, these results provide valuable information of the transient speed of solar PV output power and current. Furthermore, it can also be conclude that $|\Delta P_{boost}/\Delta t|$ is always smaller than $|\Delta P_{pv}/\Delta t|$ under the same window length which is also true for $|\Delta I_{boost}/\Delta t| < |\Delta I_{pv}/\Delta t|$. This demonstrates that the power converter used to control the solar PV output also have the capability to smooth the power and current output.

V. CONCLUSION

This paper analysed the solar irradiance intermittency characteristics within very short time periods and their impacts on the solar PV and DC/DC converter outputs. Statistical analysis of the measured solar PV irradiance data considering the distribution of intermittency and short-term irradiance ramping detection have been discussed in detail. A system level detailed simulation model has been developed and used to study various scenarios to emulate the potential impacts of the short-short term irradiance variations on a residential DC microgrid that will be studied in the future. The presented results highlight the maximum possible rate-of-change of solar PV and converter current and power outputs, i.e. $\Delta P/\Delta t$ and $\Delta I/\Delta t$. These findings provide useful insights and key considerations of sizing and designing distributed solar PV systems, more specifically about the selection of filtering capacitors. Furthermore, the paper verified that connecting the solar PV with power converters as well as well-designed control system can smooth the unexpected solar fluctuations.

Future planned work will further examine the impacts of short-term irradiance intermittency of the design of power converters as well as the power coordination problem to integrate with battery system within DC microgrids

TABLE V. MAXIMUM VARIATIONS AND RAMPING RATE OF POWER AND CURRENT UNDER DIFFERENT WINDOWS

Window size (s)	**Ramping**	ΔG (W/m^2)	ΔP_{pv} (W)	ΔP_{boost} (W)	ΔI_{pv} (A)	ΔI_{boost} (A)	$\lvert\Delta G/\Delta t\rvert$ (W/m^2/s)	$\lvert\Delta P_{pv}/\Delta t\rvert$ (W/s)	$\lvert\Delta P_{boost}/\Delta t\rvert$ (W/s)	$\lvert\Delta I_{pv}/\Delta t\rvert$ (A/s)	$\lvert\Delta I_{boost}/\Delta t\rvert$ (A/s)
2	Up	218.9	1269	1219	4.74	4.30	218.9	1269	1219	4.74	4.30
	Down	-218.8	-1318	-1259	-4.87	-4.39	218.8	1318	1259	4.87	4.39
10	Up	828.4	5141	4966	17.63	15.87	153.6	942.7	919.4	3.16	2.85
	Down	-824.4	-5137	-4940	-17.78	-16.00	171.8	1078	1030	3.78	3.40
30	Up	973.1	6017	5729	21.89	19.71	117.5	731.1	688.3	2.72	2.45
	Down	-964.3	-5933	-5661	-21.42	-19.28	115.5	716.9	673.3	2.70	2.43
60	Up	1013.0	6322	6047	22.41	20.17	112.8	698.1	672.6	2.39	2.16
	Down	-1012.0	-6175	-5961	-21.54	-19.38	163.6	979.6	953.7	3.32	3.00

REFERENCES

[1] Australian Energy Market Operator, "2022 Integrated System Plan," 2022.

[2] Y. Huo, and G. Gruosso, "A novel ramp-rate control of grid-tied PV-Battery systems to reduce required battery capacity," *Energy*, vol. 210, pp. 118433, 2020/11/01/, 2020.

[3] D. S. Kumar, S. Maharjan, Albert, and D. Srinivasan, "Ramp-rate limiting strategies to alleviate the impact of PV power ramping on voltage fluctuations using energy storage systems," *Solar Energy*, vol. 234, pp. 377-386, 2022/03/01/, 2022.

[4] L. Polleux, G. Guerassimoff, J.-P. Marmorat, J. Sandoval-Moreno, and T. Schuhler, "An overview of the challenges of solar power integration in isolated industrial microgrids with reliability constraints," *Renewable and Sustainable Energy Reviews*, vol. 155, pp. 111955, 2022/03/01/, 2022.

[5] J. Traube et al., "Mitigation of Solar Irradiance Intermittency in Photovoltaic Power Systems With Integrated Electric-Vehicle Charging Functionality," *IEEE Transactions on Power Electronics*, vol. 28, no. 6, pp. 3058-3067, 2013.

[6] T. Schittekatte et al., "The Impact of Short-Term Stochastic Variability in Solar Irradiance on Optimal Microgrid Design," *IEEE Transactions on Smart Grid*, vol. 9, no. 3, pp. 1647-1656, 2018.

[7] J. Mossoba et al., "Analysis of solar irradiance intermittency mitigation using constant DC voltage PV and EV battery storage," *2012 IEEE Transportation Electrification Conference and Expo (ITEC)*, 2012, pp. 1-6, doi: 10.1109/ITEC.2012.6243473.

[8] T.-T. Ku, and C.-S. Li, "Implementation of Battery Energy Storage System for an Island Microgrid With High PV Penetration," *IEEE Transactions on Industry Applications*, vol. 57, no. 4, pp. 3416-3424, 2021.

[9] R. B. Hytowitz, and K. W. Hedman, "Managing solar uncertainty in microgrid systems with stochastic unit commitment," *Electric Power Systems Research*, vol. 119, pp. 111-118, 2015/02/01/, 2015.

[10] G. Haines, N. Ertugrul, G. Bell, and M. Jansen, "Microgrid system and component evaluation: Mobile test platform with battery storage." *2017 IEEE Innovative Smart Grid Technologies - Asia (ISGT-Asia)*, 2017, pp. 1-5, doi: 10.1109/ISGT-Asia.2017.8378466.

[11] Gilman, P.; Dobos, A.; DiOrio, N.; Freeman, J.; Janzou, S.; Ryberg, D. (2018) SAM Photovoltaic Model Technical Reference Update. 93 pp.; NREL/TP-6A20-67399.

[12] S. K. Kollimalla and M. K. Mishra, "Variable Perturbation Size Adaptive P&O MPPT Algorithm for Sudden Changes in Irradiance," in *IEEE Transactions on Sustainable Energy*, vol. 5, no. 3, pp. 718-728, July 2014, doi: 10.1109/TSTE.2014.2300162.

[13] Y. Yao, N. Ertugrul and S. A. Pourmousavi, "Power Sharing and Voltage Regulation in Islanded DC Microgrids with Centralized Double-Layer Hierarchical Control," *2021 31st Australasian Universities Power Engineering Conference (AUPEC)*, 2021, pp. 1-6, doi: 10.1109/AUPEC52110.2021.9597804.